Locally Self-Consistent Green's Function Method and Its Application in the Theory of Random Alloys

I. A. Abrikosov, P. A. Korzhavyi, and B. Johansson

Condensed Matter Theory Group, Physics Department,
Uppsala University, S-75121 Uppsala, Sweden

Abstract. A formulation of the order-N locally self-consistent Green's function, LSGF, method in conjunction with the linear muffin-tin orbital (LMTO) basis set is discussed. The method is particularly suitable for calculating the electronic structure of systems with an arbitrary distribution of atoms of different kinds on an underlying crystal lattice. We show that in the framework of the tight-binding representation it can be generalized to systems without ideal three-dimensional symmetry of the underlying lattice, like, for instance, alloys with local lattice relaxations or surface alloys. We also show that multipole corrections to the atomic sphere approximation can be easily incorporated into the formalism. Thus, the method represents a powerful tool for studing different problems within alloy theory.

1 Introduction

Recent research in solid state physics has shown a number of encouraging results for the investigation of physical properties of metallic alloys. In particular, the computational schemes which allow one to treat ordered, as well as random alloys, their surfaces and interfaces have been developed and applied with a great success. This has led to a much deepened understanding of the behavior of thermodynamic and magnetic properties, structural and phase stabilities, impurity, surface and segregation energies through the transition metal series [1–5]. On the other hand, first-principles investigations are still limited to certain ideal systems, like, for instance, completely ordered or completely random alloys, while for materials and problems of technological importance these studies are quite rare. A possible improvement of this circumstance consists in the development of more efficient computational schemes, for example, methods that scale linearly with increasing number of atoms in the system (order-N methods), thereby allowing a study of more realistic systems.

The problem is schematically illustrated in Fig. 1. In the framework of density functional theory (DFT) [6] our purpose is to solve the Kohn-Sham equations [7] for an infinite system of atoms. This set of effective one-electron equations is conventionally solved with a particular choice of basis functions. However, such an approach relies on the Bloch theorem, and thus requires ideal three-dimensional periodicity of the system at hand. If this is not the case, the periodicity is usually imposed artificially by considering only a finite part of the original system, the

H. Dreyssé (Ed.): Workshop 1998, LNP 535, pp. 379–398, 1999.

so called supercell, subject to periodic boundary conditions (Fig. 1a). This allows one to construct a Hamiltonian matrix which upon Fourier transformation to reciprocal k-space has a dimension proportional to the number of atoms N in the supercell. But due to the famous $O(N^3)$ scaling problem (i.e. the computational time increases as N^3 with the number of atoms N in the supercell) the size of the cell is often limited by the computer power rather than by the physical problem itself. On the other hand, to account for short range order effects in alloys [8,9] or to calculate interaction energies between point defects in a metal [10] one needs supercells with more than a hundred of atoms. For such big supercells conventional approaches are not at all efficient, and scaling properties of the computational technique must be improved.

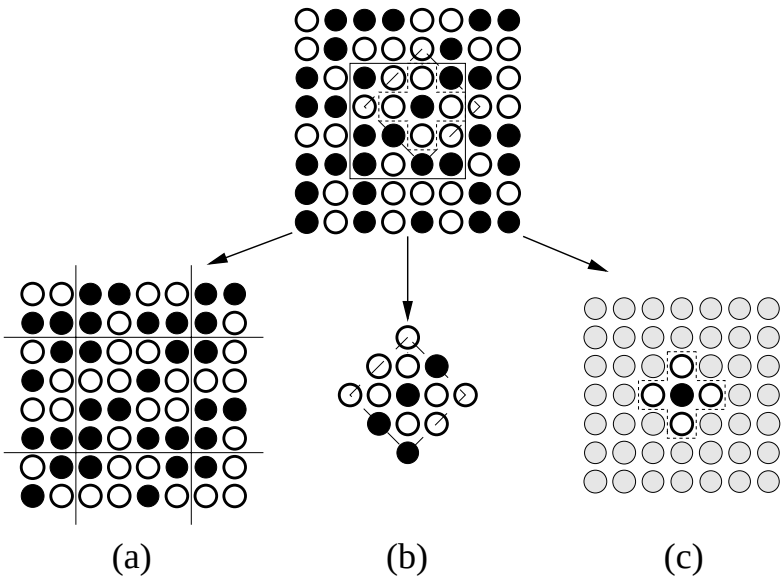

Fig. 1. Three ways to calculate electronic structure of infinite system composed of chemically nonequivalent atoms (*filled and open circles*) with an arbitrary degree of disorder. (**a**) In the framework of the supercell method one chooses some part of the original system (indicated by a *full line*), and repeats it periodically. (**b**) Conventional $O(N)$ methods are based on the direct solution of the electronic structure problem for a finite part of the original system (*dashed line*), the local interaction zone, centered at all the sites of this system. (**c**) Within the LSGF method the boundary conditions for the multiple scattering problem inside a LIZ are substantially improved by embedding the LIZ into a self-consistent effective medium (*gray circles*). As a result the size the LIZ is greatly reduced (*dotted line*)

Within the last decade considerable attention has been devoted to the development of so-called $O(N)$ methods. Most of them are based on the principle of

nearsightedness [11], illustrated in Fig. 1b. Similar to the supercell method, one considers a finite subsystem of the original system, the so called local interaction zone (LIZ) [12,13]. But rather than introducing periodic boundary conditions, one solves the electronic structure problem for the particular LIZ, and then proceeds to the next LIZ, thus dividing the N-atom problem into N more or less independent problems for each LIZ. Such a procedure can be partly justified by the experience gained in the application of real-space cluster methods in electronic structure calculations that shows that for a large cluster the properties of an atom deep inside the cluster are very close to those given by band structure methods. Also, it guarantees linear scaling of the computational efforts with N.

Several $O(N)$ computational techniques differ from each other mainly by the methods of solving the electronic structure problem for the LIZ. For example, in Refs. [14–18] this is done by employing localized orbitals, Refs. [19–23] take advantages of the density matrix formulation, in Refs. [24,25] tigh-binding (TB) representation is used, while the techniques presented in Refs. [12,13,26,27] are based on a Green's function approach. However, if there are M atoms in the LIZ, then the computational effort required for an exact solution of the electronic structure problem inside a particular LIZ scales as M^3. Thus the total computational time scales as M^3N. One can see from Fig. 2 that there is a certain minimum number of atoms $\tilde{N}$ for which the $O(N)$ methods become more efficient than conventional $O(N^3)$ methods. Thus, the problem with $O(N)$ methods is not only to achieve the linear scaling of the computational efforts with increasing number of atoms, but also to minimize the size of the LIZ. Unfortunately, applications of the above mentioned linear scaling methods are very limited due to the fact that the size of their LIZ must in general be chosen quite large to give reliable description of the electronic properties, especially for metals [12,13].

The origin of this drawback can be understood as follows. From an illustration in Fig. 1b one can see that all the information about the system beyond the LIZ is totally neglected. Therefore, one needs to keep too many atoms directly in the LIZ in order not to loose essential physical information about the original system. Thus, there is a question if one can make the central atom of the LIZ more nearsighted. In Refs. [8,28] we have suggested that one can do this if one keeps at least some information about the system beyond the truncation region in the form of an effective medium (Fig. 1c). And, of course, the more information is kept, the better the convergence will be with respect to the size of the LIZ. Therefore, we have suggested to choose the effective medium that describes properties of the original system on average as accurate as possible. It is also clear that the symmetry of the effective medium may be much higher than the symmetry of the system under consideration. In Refs. [8,28] we have demonstrated how the computational effort of $O(N)$ calculations may be considerably reduced by embedding the LIZ in this effective medium (see Fig. 1c). Such an embedding may be established by means of the Dyson equation connecting the desired Green's function to the Green's function of the reference system.

In the present paper we first review the main ideas of the locally self-consistent Green's function (LSGF) technique proposed by Abrikosov *et al.* [8,28]. We then

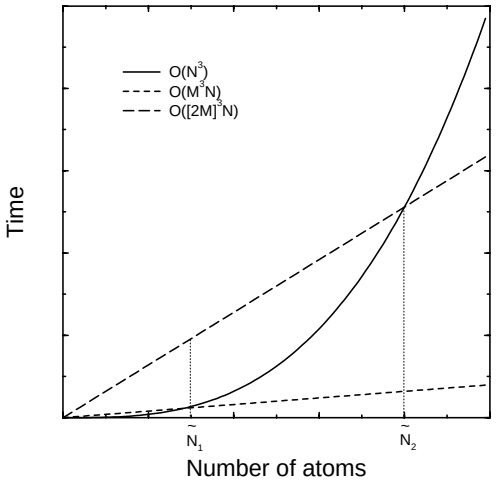

Fig. 2. Schematic representation of computational efforts required to solving the electronic structure problem by a conventional $O(N^3)$ method (*full line*), as well as by $O(N)$ methods with different number of atoms, M (*dashed line*) and $2M$ (*long-dashed line*), in the local interaction zone

discuss some resent developments, in particular, multipole corrections to the atomic sphere approximation (ASA) [29,30] for the one-electron potential. We will next show how the tight-binding representation of the linear muffin-tin orbital method [31–35] can be incorporated in our Green's function technique. This will allow us to formulate general equations for systems without ideal three-dimensional symmetry of the underlying lattice, like, for instance, alloys with local lattice relaxations or surface alloys. Applications of the LSGF method to several problems of solid state physics will also be briefly discussed.

2 Locally Self-Consistent Green's Function Method

2.1 Assumptions and Definitions

We will formulate the locally self-consistent Greens function method in the framework of the density functional theory and the local spin density approximation (LSDA) [6,7] in conjunction with a linear muffin-tin orbitals basis in the atomic sphere approximation of Andersen [31–35] including multipole correction terms [29,30], ASA+M. In this section we will consider the problem of calculating the electronic structure of a system of N atoms illustrated in Fig. 1. Though this is not necessary, we assume that the original system is represented by a supercell subjected to periodic boundary conditions. This assumption allows us to calculate easily the long-ranged electrostatic contributions to the one-electron

potential and energy, and to construct appropriate LIZ for atoms close to the boundary of the supercell. We allow for an arbitrary distribution of the atoms that may be of different types on the sites of the underlying crystal lattice. However, in this section we do not allow these lattice sites to deviate from their ideal positions, i.e. we neglect the so-called local relaxation effects. This problem will be considered in Sec. 3.2.

We will assign to each site of the supercell a corresponding atomic sphere (AS) centered at radius-vector $\mathbf{R}$. Inside each AS we will define the electron density $\rho_{\mathbf{R}}(\mathbf{r})$ and one-electron potential $v_{\mathbf{R}}(\mathbf{r})$. Also the potential function $P^{\alpha}_{\mathbf{R}l}(z)$

$$P^{\alpha}_{\mathbf{R}l}(z) = \frac{z - C_{\mathbf{R}l}}{(z - C_{\mathbf{R}l})(\gamma_{\mathbf{R}l} - \alpha_l) + \Delta_{\mathbf{R}l}} \tag{1}$$

for an arbitrary (complex) energy z and angular-momentum quantum number l may be assigned to each site. It is expressed by means of the band center C, bandwidth Δ, and the γ LMTO potential parameters calculated at an arbitrary energy $\varepsilon_{\nu\mathbf{R}l}$ in the energy range of interest [33]. Index α denotes the LMTO representation, and in the following discussion it will be used only when relevant. The so-called KKR-ASA Green's function matrix $\mathbf{g}$ is defined like

$$[\mathbf{P}(z) - \mathbf{S}(\mathbf{k})]\mathbf{g}(\mathbf{k}, z) = \mathbf{1}, \tag{2}$$

where $\mathbf{P}, \mathbf{S}$ and $\mathbf{g}$ are $(\mathbf{R}L, \mathbf{R}'L')$ matrices, L is the combined angular-momentum quantum numbers (l, m), and the structure constant matrix $\mathbf{S}$ contains all the information about the crystal structure. The real space KKR-ASA Green's function matrix $g_{\mathbf{R}L,\mathbf{R}'L'}(z)$ is obtained from $\mathbf{g}(\mathbf{k})$ by integration over the Brillouin zone

$$g_{\mathbf{R}L,\mathbf{R}'L'}(z) = (V_{BZ})^{-1} \int_{BZ} d\mathbf{k}\, e^{\mathrm{i}\mathbf{k}\cdot(\mathbf{T}-\mathbf{T}')} g_{\mathbf{U}L,\mathbf{U}'L'}(\mathbf{k}, z), \tag{3}$$

where V_{BZ} is the volume of the Brillouin zone, $\mathbf{U}$ is a basis vector of the unit cell. It is connected to the lattice site $\mathbf{R}$ by a translation $\mathbf{T}$, i.e., $\mathbf{R} = \mathbf{U} + \mathbf{T}$. The on-site element $g_{\mathbf{R}L,\mathbf{R}L'}(z)$ is a key quantity which determines both the electron density and the density of states at the $\mathbf{R}$-th site. Therefore, our purpose is to calculate these matrix elements for all the sites of the supercell. In a conventional Green's function technique this requires an inversion of Eq. (2) at each k-point in the Brillouin zone and for each energy point z. This is essentially the operation that results in $O(N^3)$ scaling of the problem. In the following we will show how this problem can be solved without a direct inversion of Eq. (2) in the framework of the LSGF method.

2.2 Concept of Local Self-Consistency and Effective Medium

The concept of local self-consistency is based on the suggestion that the electron density and the density of states on a particular atom within a large condensed

system may be obtained with sufficient accuracy by considering only the electronic multiple scattering processes in a finite spatial region centered at that atom. This concept has been applied by by Nicholson *et al.* [12,13] in the framework of the locally self-consistent multiple scattering (LSMS) method. Within this method each atom of a system is surrounded by few shells of nearest neighbors (see Fig. 1b), the local interaction zone, and the multiple scattering problem is solved in the real space for each LIZ independently of the other LIZs. The method was proven to have essentially $O(N)$ scaling properties with increasing supercell size. Nevertheless, it turns out that the minimal size of the LIZ should be about 100 atoms and even more to provide the accuracy of order 0.1 $mRy/atom$ for the total energy. It is quite clear that the reliable description of the central site scattering properties will be achieved only when the size of the LIZ is so large, that an atom at this site becomes completely insensitive to what is happening beyond the LIZ. In particular, if one adds an extra atom at the LIZ's boundary, this should have no effect on the central site.

The concept of local self-consistency has been further developed by Abrikosov *et al.* [8,28] in the locally self-consistent Green's function method (LSGF), where the concept of an effective medium has been combined together with the LIZ concept. This resulted in the development of an efficient $O(N)$ technique. The combination of these two concepts can be most easily illustrated by the example of a substitutional alloy with an arbitrary degree of short and long range order.

In choosing the effective medium we tried to satisfy the following main criteria, namely its scattering properties as viewed by the central atom of the LIZ must be as close as possible to those of the original system at the shortest possible distance. Additionally, it has to be as simple (i.e. symmetric) as possible. In the case of the above mentioned substitutional alloy it is clear that a very good representation of the real system beyond the LIZ would be a completely random alloy. In particular, one can expect that the convergence with respect to the LIZ size will be achieved as soon as the central site becomes insensitive to the interchange of positions of two atoms at the LIZ's boundary, in contrast to a requirement of the complete insensitivity in conventional $O(N)$ schemes. Also, the random alloy has on the average the highest possible symmetry, and this will allow us to perform at least partly calculations in the reciprocal space of the effective lattice which in its own turn has a minimal number of atoms in the unit cell.

Now, there is a question of how to represent mathematically the effective medium in the form of a completely random alloy. Based on the experience gained in the study of alloys Abrikosov *et al.* [8,28] have suggested to do this in the framework of the multicomponent generalization of the coherent-potential approximation (CPA). In fact, the CPA effective medium fulfills both the above mentioned criteria. Despite the fact that the CPA is a very simple single-site approximation, it has been shown to give density of states for random alloys in very good agreement with experiment as well as with more accurate calculations that go beyond the single-site approximation [36–38]. In addition, the

CPA Green's function decays, apart from an oscillating factor, exponentially as $R^{-1}e^{-R/l}$, where l is the mean free path [2].

However, conventionally the CPA describes scattering property of a binary alloy in terms of two potentials, for A and B alloy component. In reality situation is different, and in a N atom system, even though it is composed of just two chemically inequivalent atoms, A and B, all the local potentials are in general inequivalent due to the differences in local environments of any site. Therefore, one must define the effective medium to be used in the embedding of the LIZ as that given by the CPA for a multicomponent alloy. The number of components at each sublattice will be equal to the number of equivalent positions in the supercell formed from the underlying lattice, i.e., in the simplest case of a monoatomic underlying lattice each atom in the supercell is considered to be a component of an N-atom alloy. We thereby assume that the atoms are randomly distributed on their sublattices and neglect the fact that they occupy definite positions in the system. The difference between different atoms (or alloy components) will enter through their one-electron potentials. This method has recently been elevated to an idea of polymorphous CPA [38].

2.3 Computational Algorithm

In this section we will describe in details the complete self-consistent procedure of the LSGF method within the LMTO basis set as applied to the problem of calculating the electronic properties of a paramagnetic system of N atoms in a supercell subjected to periodic boundary conditions, such as illustrated in Fig. 1. Generalization to systems with collinear magnetic moments is straightforward, but there also exists a generalization of the method for systems with arbitrary orientations of local magnetic moments [39].

The principal scheme is similar to any other Green's function technique [34,40–43], but there are certain new steps that are specific for the LSGF method. We start with a guess for the charge density of all the atoms in the system, calculated as a renormalized atomic density or by means of a conventional CPA calculation for a random alloy with the same composition as in the supercell. The first problem is to construct an effective medium (all parameters that characterize the latter are denoted by a tilde). This means we must determine the potential function for the effective scatterers $\tilde{P}$ and the effective Green's function $\tilde{g}$. Here we remark, that in some cases it turns out to be more efficient to chose the effective medium in the form of multisublattice alloy. In particular, it has been demonstrated in Ref. [28] that for a partially ordered $\mathrm{Ni(Ni_{9.375}Al_{90.625})}$ alloy the convergence with respect to the size of the LIZ is substantially enhanced by substituting the most symmetric bcc effective medium for an effective medium on B2 underlying lattice with two nonequivalent types of the effective atoms, one for each nonequivalent sublattice. Thus, one must solve the following system of coupled single-site equations for the $\tilde{\mathbf{U}}$ sites in the unit cell of the underlying lattice [43,44]

$$\begin{aligned}
\tilde{g}_{\tilde{\mathbf{U}}\tilde{\mathbf{U}}} &= (\tilde{V}_{BZ})^{-1} \int_{BZ} d\mathbf{k}\, ([\tilde{\mathbf{P}} - \tilde{\mathbf{S}}(\mathbf{k})]^{-1})_{\tilde{\mathbf{U}}\tilde{\mathbf{U}}} \\
g^0_{\mathbf{R}} &= \tilde{g}_{\tilde{\mathbf{U}}\tilde{\mathbf{U}}} + \tilde{g}_{\tilde{\mathbf{U}}\tilde{\mathbf{U}}}(\tilde{P}_{\tilde{\mathbf{U}}} - P_{\mathbf{R}}) g^0_{\mathbf{R}} \\
\tilde{g}_{\tilde{\mathbf{U}}\tilde{\mathbf{U}}} &= (N_{\tilde{\mathbf{U}}})^{-1} \sum_{\mathbf{R}} g^0_{\mathbf{R}},
\end{aligned} \tag{4}$$

where $\tilde{\mathbf{U}}$ denotes a particular sublattice of the underlying lattice, $\mathbf{R} \in \tilde{\mathbf{U}}$, i.e., $\mathbf{R} = \tilde{\mathbf{U}} + \tilde{\mathbf{T}}$, $\tilde{V}_{BZ}$ is the volume of the Brillouin zone of the underlying unit cell and the integration is performed over the corresponding Brillouin zone, $\tilde{\mathbf{S}}$ is the structure constant matrix of the underlying lattice. In Eq. (4) $N_{\tilde{\mathbf{U}}}$ is a number of atoms at the corresponding sublattice of the effective lattice, i.e. $N_{\tilde{\mathbf{U}}} = N$ for a Bravais lattice, while, for instance, for the B2 lattice $N_{\tilde{\mathbf{U}}} = N/2$. Eq. (4) must be solved for each sublattice of the effective lattice. In practice it is solved by iterations with an initial guess for the effective potential function in the following form:

$$\tilde{P}^{-1}_{\tilde{\mathbf{U}}} = (N_{\tilde{\mathbf{U}}})^{-1} \sum_{\mathbf{R} \in \tilde{\mathbf{U}}} P^{-1}_{\mathbf{R}} \tag{5}$$

using an efficient procedure described in details in Ref. [28].

As has been specified in Sec. 2.1, the key quantity to be calculated in order to get access to all the electronic properties of a system is on-site elements of the Green's function matrix, $g_{\mathbf{R}L,\mathbf{R}L'}(z)$. In the framework of the LSGF method we calculate them using the concept of the local self-consistency, i.e. for each site of the supercell separately. This site is considered as a central site of a corresponding LIZ embedded in the effective medium constructed by the procedure described above (Fig 1c). The Green's function for the LIZ can be found by solving corresponding Dyson equation

$$g_{\mathbf{RR}} = \tilde{g}_{\mathbf{RR}} + \sum_{R'=1}^{M} \tilde{g}_{\mathbf{RR}'}(\tilde{P}_{\mathbf{R}'} - P_{\mathbf{R}'}) g_{\mathbf{R}'\mathbf{R}}, \tag{6}$$

where the sum runs over the M atoms in the LIZ around site $\mathbf{R}$. Eq. (6) has to be solved for all the sites in the original system. Thus, the problem of solving the Kohn-Sham equations for an N-atom system is decomposed into N linked locally self-consistent problems for the LIZ associated with each atom in the system. Note also that in Eq.(6) $\tilde{g}_{\mathbf{RR}'}$ is a matrix element of the complete (diagonal, as well as off-diagonal) Green's function matrix of the effective medium, and it is calculated from the corresponding Brilluoin zone integral, Eq. (3), where $\mathbf{U}$ now represents a basis vector of the underlying lattice $\tilde{\mathbf{U}}$. At each iteration and for any energy point this Green's function must be calculated only once for the entire system, and shall not be updated when moving the LIZ from one site

to another due to the invariance of all the sites of the underlying lattice that belong to the same sublattice $\tilde{\mathbf{U}}$ with respect to a translation $\tilde{\mathbf{T}}$. Moreover, due to the high symmetry of the effective medium calculating integral (3) is not a time-consuming operation.

We remark that in general $g_{\mathbf{R}\mathbf{R}'}$ calculated by the Dyson equation (6) will not correspond to the one of a real system, especially close to the LIZ boundary. But the on-site element for the central atom will approach that of the real atom at $\mathbf{R}$ for a sufficiently large LIZ. In this sense $g_{\mathbf{R}\mathbf{R}}$ will be locally self-consistent. This also distinguishes a solution of Eq. (6) from a solution of a single-site CPA Eq. (4), thus justifying our use of different notations for the corresponding on-site elements of the Green's function in these equations.

After the on-site elements of the Green's function have been calculated for the entire system, i.e. Eq. (6) has been solved for all the sites $\mathbf{R}$, the remaining procedure is completely similar to any conventional Green's function technique [34,40–43]. We proceed by transforming the KKR-ASA Green's function g into the Hamiltonian Green's function G:

$$G^{\gamma}_{\mathbf{R}L,\mathbf{R}L'}(z) = \frac{1}{z - V^{\alpha}_{\mathbf{R}l}}\delta_{LL'} + \frac{\sqrt{\Gamma^{\alpha}_{\mathbf{R}l}}}{z - V^{\alpha}_{\mathbf{R}l}} g^{\alpha}_{\mathbf{R}L,\mathbf{R}L'}(z) \frac{\sqrt{\Gamma^{\alpha}_{\mathbf{R}l'}}}{z - V^{\alpha}_{\mathbf{R}l'}}, \tag{7}$$

where the LMTO-representation dependent potential parameters $V^{\alpha}_{\mathbf{R}l}$, $\Gamma^{\alpha}_{\mathbf{R}l}$ are

$$\begin{aligned} V^{\alpha}_{\mathbf{R}l} &= C_{\mathbf{R}l} - \frac{\Delta_{\mathbf{R}l}}{\gamma_{\mathbf{R}l} - \alpha_l} \\ \Gamma^{\alpha}_{\mathbf{R}l} &= \frac{\Delta_{\mathbf{R}l}}{(\gamma_{\mathbf{R}l} - \alpha_l)^2}. \end{aligned} \tag{8}$$

Then the moments of the state density can be calculated

$$m^{q'q''}_{\mathbf{R}L'L''} = \frac{1}{2\pi i} \oint dz (z - \varepsilon_{\nu\mathbf{R}l'})^{q'} G^{\gamma}_{\mathbf{R}L',\mathbf{R}L''}(z) (z - \varepsilon_{\nu\mathbf{R}l''})^{q''} \tag{9}$$

and using the second-order Taylor expansion of the partial wave, $\phi_{\mathbf{R},l}(\varepsilon; r)$:

$$\phi_{\mathbf{R}l}(\varepsilon; r) \approx \phi_{\nu\mathbf{R}l}(r) + \ (\varepsilon - \varepsilon_{\nu\mathbf{R}l})\ \dot{\phi}_{\nu\mathbf{R}l}(r) + \frac{1}{2}(\varepsilon - \varepsilon_{\nu\mathbf{R}l})^2\ \ddot{\phi}_{\nu\mathbf{R}l}(r), \tag{10}$$

the valence charge density $n^{v}_{\mathbf{R}}(r)$ in the corresponding atomic spheres can be found as the one-centre expansion

$$\begin{aligned} n^{v}_{\mathbf{R}}(r) = (4\pi)^{-1} \sum_{L} \{ & [\phi_{\nu\mathbf{R}l}(r)]^2 m^{00}_{\mathbf{R}LL} + 2[\phi_{\nu\mathbf{R}l}(r)\dot{\phi}_{\nu\mathbf{R}l}(r)] m^{10}_{\mathbf{R}LL} \\ & + [\dot{\phi}_{\nu\mathbf{R}l}(r)\dot{\phi}_{\nu\mathbf{R}l}(r) + \phi_{\nu\mathbf{R}l}(r)\ddot{\phi}_{\nu\mathbf{R}l}(r)] m^{20}_{\mathbf{R}LL} \}. \end{aligned} \tag{11}$$

In Eq. (9) the contour must enclose the occuped valence states, while $\phi_{\nu\mathbf{R}l}$, $\dot{\phi}_{\nu\mathbf{R}l}$, and $\ddot{\phi}_{\nu\mathbf{R}l}$ in Eqs. (10) and (11) denote the partial wave and its first and second energy derivatives, respectively, evaluated at the energy $\varepsilon_{\nu\mathbf{R}l}$. An iteration is completed by solving Poissons equation for the electrostatic potential and adding the exchange-correlation potential. In addition, in contrast to the conventional treatment of an alloy problem in the framework of the CPA, adding corrections to the ASA becomes meaningful within the LSGF scheme. This will be described in the next section. The entire procedure is then repeated until self-consistency.

2.4 Multipole Corrections to the ASA

A supercell approach allows one to calculate the electrostatic contributions to the one-electron potential and energy exactly by performing the Madelung summation, because the atomic sphere charges in that case are calculated explicitly [12,13,8]. However, in the ASA, the electron charge is usually assumed to have spherical symmetry inside each atomic sphere. This approximation works quite well if all the atomic positions have high-symmetry local coordinations. When the local symmetry is broken, this approximation becomes less appropriate, and calculations based on the atomic sphere approximation sometimes lead to substantial errors when calculating physical properties of solids. For example, the vacancy formation energy is usually overestimated by as much as a factor of 2 [45–47], and the work function is about 50 % higher than experimental values [29,4].

The problem of Madelung contributions naturally emerges if one divides the crystal space into atomic or muffin-tin spheres and tries to describe the electrostatic interaction between the interior of a sphere and the rest of the crystal by adding a certain, constant throughout the sphere, electrostatic shift to the one-electron potential. However, if one considers, for example, an isolated vacancy in a metal matrix, then one sees that vacancy itself has a very symmetrical local coordination in the case of a cubic or hexagonal crystal structure of the metal matrix. But the local coordination of its close neighbors is very unsymmetrical because one atom has been removed to form the vacancy. On each of the vacancy neighbors a dipole moment of the electron charge should appear as a result of the fact that atomic density tails penetrate into this atomic sphere from all of its neighbors except the vacant site. An additional monopole potential shift on the vacant site must be thus induced by the dipole moments of the surrounding atoms. It is clear, that this contribution is omitted if the spherical approximation for the electron density is used.

This simple example illustrates the importance of taking into account multipole Madelung contributions to the potential and energy when dealing with a system in which the symmetry of the local configurations is low. Otherwise, the system can be adequately described by only the monopole Madelung terms. It is, of course, also important to examine the relative contributions of the multipoles higher than the dipole, but it is clear that the dipole term is dominant in the case of a vacancy as well as for surface problems.

Probably the most consistent way of dealing with this problem would be in the framework of a full-potential approach. However, as has been shown in several works [29,4,48,49,30], one can expect to be able to determine an accurate total energy of a system by still using a spherical potential provided the spherical approximation to the electron charge density is lifted. The monopole ($L = 0$) Madelung contribution to the one-electron potential is then evaluated using the monopole as well as multipole components of the valence electron charge, $Q_L^{\mathbf{R}}$, as:

$$V_0^{\mathbf{R}} = \frac{1}{S} \sum_{\mathbf{R}',L'} M_{0L'}^{\mathbf{R}\mathbf{R}'} \; Q_{L'}^{\mathbf{R}'}, \tag{12}$$

where $M_{LL'}^{\mathbf{R}\mathbf{R}'}$ is the multipole Madelung matrix which is equivalent to the conventional (unscreened) LMTO structure constants for the *entire* supercell, and S is the average Wigner-Seitz radius in all space.

On the other hand, the total energy is calculated including all possible electrostatic interactions between the multipole charges (monopole - monopole, monopole - dipole, dipole - dipole, etc.):

$$E_M = \frac{1}{2S} \sum_{\mathbf{R},L} Q_L^{\mathbf{R}} \sum_{\mathbf{R}',L'} M_{LL'}^{\mathbf{R}\mathbf{R}'} \; Q_{L'}^{\mathbf{R}'}. \tag{13}$$

In Eqs. (12) and (13) multipole moments of the charge density are calculated as integrals over the atomic sphere with the origin taken at $\mathbf{R}$:

$$\begin{aligned} Q_L^{\mathbf{R}} &= \frac{\sqrt{4\pi}}{2l+1} \int_{\mathbf{R}} d\mathbf{r} \; Y_L^*(\hat{\mathbf{r}}) \left(\frac{r}{S_{\mathbf{R}}}\right)^l n_{\mathbf{R}}(\mathbf{r}) - Z_{\mathbf{R}}\delta_{l,0} \\ &= \frac{\sqrt{4\pi}}{2l+1} \sum_{L',L''} C_{L,L',L''} \int_0^{S_{\mathbf{R}}} dr \left(\frac{r}{S_{\mathbf{R}}}\right)^l r^2 f_{\mathbf{R}L'L''}(r) - Z_{\mathbf{R}}\delta_{l,0}. \end{aligned} \tag{14}$$

Here $S_{\mathbf{R}}$, $n_{\mathbf{R}}(\mathbf{r})$ and $Z_{\mathbf{R}}$ are the atomic sphere radius, valence (nonspherical) electron density and valence number, respectively, of the atom at the site $\mathbf{R}$, $Y_L(\hat{\mathbf{r}})$ is a real harmonic, and $C_{L,L',L''}$ are real-harmonic Gaunt coefficients. Radial parts of the valence density, $f_{\mathbf{R}L'L''}(r)$, are obtained using the second-order Taylor expansion of the partial wave (10) as

$$\begin{aligned} f_{\mathbf{R}L'L''} = {} & \phi_{\nu\mathbf{R}l'}\phi_{\nu\mathbf{R}l''} m_{\mathbf{R}L'L''}^{00} + \; \phi_{\nu\mathbf{R}l'}\dot{\phi}_{\nu\mathbf{R}l''} m_{\mathbf{R}L'L''}^{01} \\ & + \dot{\phi}_{\nu\mathbf{R}l'}\phi_{\nu\mathbf{R}l''} m_{\mathbf{R}L'L''}^{10} \; + \dot{\phi}_{\nu\mathbf{R}l'}\dot{\phi}_{\nu\mathbf{R}l''} m_{\mathbf{R}L'L''}^{11} \\ & + \frac{1}{2}\phi_{\nu\mathbf{R}l'}\ddot{\phi}_{\nu\mathbf{R}l''} \; m_{\mathbf{R}L'L''}^{02} + \; \frac{1}{2}\ddot{\phi}_{\nu\mathbf{R}l'}\phi_{\nu\mathbf{R}l''} \; m_{\mathbf{R}L'L''}^{20}. \end{aligned} \tag{15}$$

In the last expression, the radial dependence of $f_{\mathbf{R}L'L''}(r)$ and the expansion coefficients $\phi_{\nu\mathbf{R}l}(r)$ has been omitted. In Eq. (15) the density of states moments,

$m^{q'q''}_{\mathbf{R}L'L''}$, are given by Eq. (9). In this regard we remark that if the angular momentum cutoff for the Green's function is equal to l_{max}, then multipole moments of the charge density, Eq. (14), have nonzero components up to $2l_{max}$ due to the properties of Gaunt coefficients.

3 Taking Advantages of Tight-Binding LMTO Representation

All equations presented in Sec. 2 are formulated for a general LMTO representation α. Indeed, in the case of a bulk alloy without local lattice relaxations LSGF calculations can be carried out in any representation with the same computational efforts. However, when in addition to a substitutional disorder the ideal three-dimensional symmetry of an underlying lattice is also broken, a formulation of the method in terms of tight-binding (TB) LMTO basis set can give one a substantial advantage. Below we will consider two such cases, that is we will present generalization of the LSGF method to the case of (i) a surface alloy and (ii) an alloy with local distortions of atomic positions from the sites of ideal underlying lattice (local lattice relaxations).

3.1 Electronic Properties of Surface Alloys: the LSGF Method

The large interest in theoretical investigations of surfaces of transition metals and their alloys is motivated by its fundamental scientific value, as well as by the great practical importance of these systems. The properties of solid surfaces and interfaces between two metals play an important role in such phenomena as catalysis, chemisorbtion, adhesion and corrosion, just to mention a few examples. Recently there has been significant progress in *ab initio* calculations of the electronic structure of surfaces of ordered materials using first-principles techniques. It appears that one may calculate surface related properties such as surface tension and work function with a high degree of accuracy [29,4]. In this context, random metallic alloys represent a large class of important materials. As to now the surface properties of these systems have only been investigated in a few cases.

Let us consider for simplicity a system of N atoms with an ideal surface, i.e. without any imperfections, like, for example, relaxation, reconstruction, steps, etc. (generalization of the method for the latest case is trivial). The system is schematically illustrated in Fig. 3. In general, there are at least two ways of solving the electronic structure problem for this system in the framework of the LSGF method. Firstly, one can use a traditional approach (Fig. 3a), and model this surface by a supercell or a slab, thus coming back to a three-dimensional problem that is to be solved by a conventional LSGF method (see Fig. 3b) described in Sec. 2. Such a computational scheme will, of course, scale linearly with increasing number of atoms in the supercell, and in principle, it has been already successfully applied for several systems [28,50]. However, in doing so one has to construct an effective medium that represents on the average scattering

properties of the alloy components, as well as takes into account a vacuum region modeled in the framework of LMTO-ASA method by empty spheres. Giving the fact that these properties differ considerably from each other, one will expect a substantial increase of the LIZ size.

At the same time, as has been demonstrated in Ref. [28], one of the advantages of the LSGF method is the possibility to vary the effective medium to suit a problem at hand. Thus, in a case of surface alloy the better choice of the latter will be the one with a layer dependent Green's function (Fig. 3c). This can be achieved in the framework of interface Green's function technique, proposed by Lambrecht and Andersen [51] and developed by Skriver and Rosengaard [29]. An implementation of this technique in conjunction with the CPA method has been described by Abrikosov and Skriver [43].

Similar to these techniques, a solution to the problem of calculating the electronic structure of a surface or an interface is separated into two parts. First, one must calculate the Green's function for the ideal bulk crystals on the both sides of the interface. In the case of a random alloy this has to be done by means of the LSGF method (Sec. 2) for a supercell which models the bulk alloy, i.e. without any presence of the surface or the interface. At the second stage one can construct an appropriate supercell to model a region of the alloy in the neighborhood of the interface. Note, that due to a local character of the perturbation induced by the surface or the interface, the size of this supercell along the direction perpendicular to the interface is not supposed to be too large. Proper boundary conditions will be ensured by using the bulk potential function from Eq. (4) for the effective medium outside the surface region obtained at the first stage. On the contrary, within the scheme illustrated in Fig. 3a and b, the whole problem must be solved for the same supercell which in this case should probably be quite large.

Following the main idea behind the LSGF method, we construct an effective medium for each layer Λ in the neighborhood of a surface as in the case of a multicomponent two-dimensional alloy:

$$\begin{aligned}
\tilde{g}^{\beta}_{\tilde{\Omega}\tilde{\Omega}}(z) &= (\tilde{A}_{SBZ})^{-1} \int_{SBZ} d\mathbf{k}_{\parallel}\, \tilde{g}^{\beta}_{\tilde{\Omega}\tilde{\Omega}}(\mathbf{k}_{\parallel}, z) \\
g^{\beta 0}_{\mathbf{R}} &= \tilde{g}^{\beta}_{\tilde{\Omega}\tilde{\Omega}} + \tilde{g}^{\beta}_{\tilde{\Omega}\tilde{\Omega}}(\tilde{P}^{\beta}_{\tilde{\Omega}} - P^{\beta}_{\mathbf{R}}) g^{\beta 0}_{\mathbf{R}} \\
\tilde{g}^{\beta}_{\tilde{\Omega}\tilde{\Omega}} &= (N_{\tilde{\Omega}})^{-1} \sum_{\mathbf{R}} g^{\beta 0}_{\mathbf{R}},
\end{aligned} \tag{16}$$

where $\tilde{A}_{SBZ}$ is the area of the 2D surface Brilouin zone (SBZ), $N_{\tilde{\Omega}}$ and $P^{\beta}_{\mathbf{R}}$ the number of atoms and the potential function of real atoms, respectively, at the sites $\tilde{\Omega} = (\tilde{\Omega}_{\parallel}, \tilde{\Omega}_{\perp})$ that belong to the same sublattice of the 2D unit cell of the underlying surface lattice in the Λ layer (note that there can be more than one site $\tilde{\Omega}$ in the layer Λ), $\tilde{P}^{\beta}_{\tilde{\Omega}}$ the potential function of an effective scatterer at $\tilde{\Omega}$, $\mathbf{R} \in \tilde{\Omega}$, and β denotes the most localized, tight-binding LMTO-representation [32,33] which is essential to use in the calculation of the surface Green's function

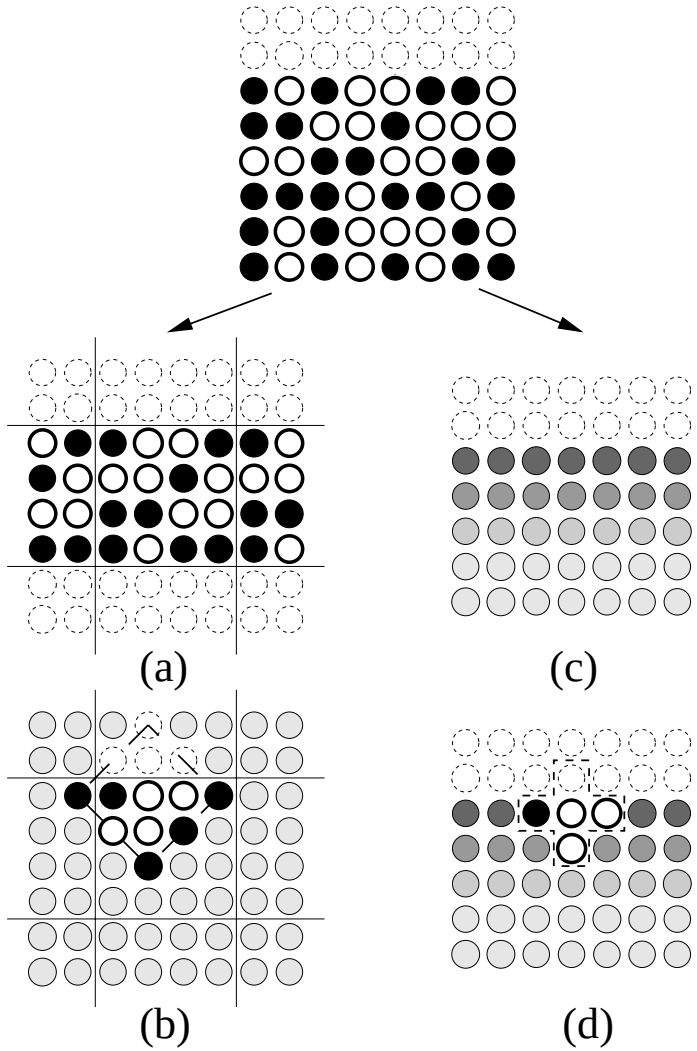

Fig. 3. Two ways of modeling surface alloy in the framework of the LSGF method. (**a**) One may employ a slab or a supercell approach, and repeat a part of the sample, including empty spheres (*thin dotted circles*) in all three directions. (**b**) An effective medium (*gray circles*) shall represent on the average scattering properties of real alloy components (*filled and open circles*), as well as empty spheres, and the embedding procedure can be carried out in a conventional manner. (**c**) By means of the interface Green's function technique in conjunction with the LSGF method the surface alloy is treated in its true semi-infinite geometry, and a layer-dependent effective medium is introduced. (**d**) Embedding procedure can be carried out, and the size of the LIZ is supposed to be smaller than in the case of the slab or the conventional supercell

$\tilde{g}^{\beta}_{\tilde{\Omega}\tilde{\Omega}}(\mathbf{k}_{\parallel}, z)$. As usual in the case of surfaces, a good quantum number is $\mathbf{k}_{\parallel} \in$ SBZ, and the dependence of the surface Green's function on $\mathbf{k}_{\perp}$ is integrated off by means of the principle layer technique [52]. In doing so one (i) calculates the ideal Green's functions for both sides of the interface using the unperturbed bulk potential functions of effective scatterers obtained for the supercell which models the *bulk* alloy, and (ii) solves a set of recurrent equations that glue the two sides of the interface together and take care of the perturbation of local potentials in the interface region. Note that this operation scales as $O(N_{\Lambda})$, where N_{Λ} is a number of layers in the interface region.

When the layer dependent effective medium is constructed by Eq. (16), i.e. $\tilde{P}^{\beta}_{\tilde{\Omega}}$ is calculated for any sublattice $\tilde{\Omega}$ and for all layers Λ in the supercell that models *surface* alloy, the embedding procedure has to be carried out in a similar manner as for the bulk alloy. If we now denote sites of the LIZ as $\mathbf{R} = (\mathbf{R}_{\parallel}, \mathbf{R}_{\perp})$, then the off-diagonal effective medium Green's function for the LIZ is calculated as an integral over the SBZ

$$\tilde{g}^{\beta}_{\mathbf{R}\mathbf{R}'}(z) = (\tilde{A}_{SBZ})^{-1} \int_{SBZ} d\mathbf{k}_{\parallel}\, e^{i\mathbf{k}_{\parallel}\cdot[(\tilde{\Omega}_{\parallel}-\tilde{\Omega}'_{\parallel})-(\mathbf{R}_{\parallel}-\mathbf{R}'_{\parallel})]} \tilde{g}^{\beta}_{\tilde{\Omega}\tilde{\Omega}'}(\mathbf{k}_{\parallel}, z), \qquad (17)$$

and the Green's function for the central site of the LIZ embedded into the effective medium (Fig. 3d) is obtained by solving Dyson equation (6). The remaining procedure is analogous to the one presented in Sec. 2.

3.2 Electronic Properties of Alloys with Local Lattice Relaxations

In general, alloys are composed of elements which are not only chemically nonequivalent, but also have different atomic sizes. As a result this size mismatch causes interatomic distancies in the alloy to be different, i.e. it causes so-called local relaxation effects. The system can also be looked upon as one where local positions of all the atoms are moved from the sites of an ideal periodic underlying lattice (Fig. 4a). Though the recent systematic study of lattice relaxations around a single impurity in Cu by Papanikolaou *et al.* [53] has shown that their contribution to the impurity solution energy in general is small compared to the values calculated earlier without lattice relaxations [3], this effect can influence the results for the density of states and the total energy calculations in some cases of very large size mismatches [54], and it is important to be able to take the local relaxations into consideration.

Within the LSGF method in conjunction with the TB-LMTO basis set the following procedure can be suggested. Firstly, we construct an effective medium for the undistorted underlying lattice in essentially the same way as has been described in Sec. 2. Then we embed a LIZ that is composed of an atom at the particular site and several shells of its nearest neighbors and that also includes all the relaxations in this effective medium (Fig. 4b). Thus, the Dyson equation that has to be solved now shall include both, the perturbation due to chemical

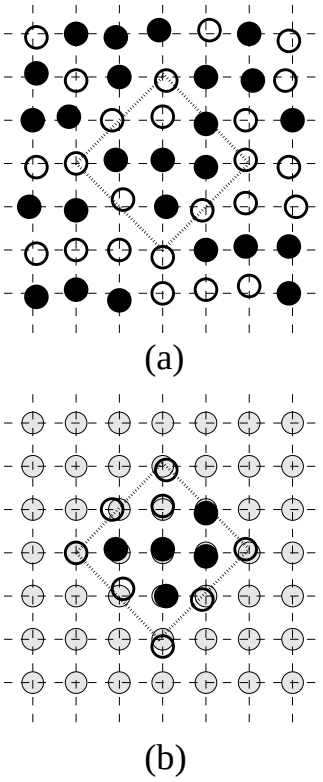

Fig. 4. Schematic representation of the LSGF method applied for an alloy with local lattice relaxations. (**a**) An original system composed of two chemically nonequivalent components (*filled and open circles*) can be looked upon as the system where local positions of all the atoms are moved from the sites of an ideal periodic underlying lattice (indicated by *thin lines*). (**b**) Effective atoms (*gray circles*) are placed at the sites of the undistorted underlying lattice, and the Dyson equation (18) for the LIZ (*dotted line*) embedded into this effective medium accounts for two kinds of perturbations, due to the potential part, as well as due to structural perturbations

disorder, as well as due to the fact that the atomic positions are shifted from the sites of the underlying lattice. In the framework of the TB-LMTO method this perturbation can be included in Eq. (6) through the difference between the real space structure constant matrices for the original system $\mathbf{S}$ and for the underlying lattice $\tilde{\mathbf{S}}$ as following

$$\mathbf{g}(z) = [(\tilde{\mathbf{g}}(z))^{-1} + (\mathbf{P}(z) - \tilde{\mathbf{P}}(z)) - (\mathbf{S} - \tilde{\mathbf{S}})]^{-1}, \tag{18}$$

where bold symbols denotes $(\mathbf{R}L, \mathbf{R}'L')$ matrices, and $\mathbf{R}, \mathbf{R}' \in$ LIZ.

Note, that the only element needed from a solution of Eq. (18) is again the on-site element $g_{\mathbf{R}L,\mathbf{R}L'}(z)$ for the central site of the LIZ. Therefore, the advantages of the TB-LMTO representation shall show up in full strength here. Not only it allows one to calculate easily structure constant matrices for the effective and the original lattices in the real space, but also due to their localized character the difference between these lattices as it is seen from the central site of the LIZ vanishes exactly at very short distancies. As has been specified in Sec. 2 the above criterion is one of the major requirements to the effective medium that ensures the minimal size of the LIZ. Therefore, though the LIZ size necessary to carry out calculations for systems with local lattice relaxations will increase compared to the unrelaxed case, this increase is not supposed to be too large.

4 Summary

The order-N locally self-consistent Green's function method has been formulated in the framework of the LMTO method in the tight-binding representation. The atomic sphere approximation has been used, but we also have shown how multipole corrections to the ASA can be easily incorporated in our formalism. The LSGF method employs two basic concepts, the local interaction zone concept, that is the multiple scattering problem is solved in real space for each atom surrounded by few shells of nearest neighbors, and the effective medium concept that provides appropriate boundary conditions for the multiple scattering problem by embedding the LIZ into a self-consistent effective medium constructed in such a way as to describe as close as possible scattering properties of the original system beyond the LIZ boundary. The latter concept ensures a minimal size of the LIZ, and therefore enhances the efficiency of the LSGF method as compared to other $O(N)$ methods. The tight-binding representation of the LMTO method allows us to present generalization of the method to two important cases, a surface alloy, and an alloy with local lattice relaxations.

Applications of the LSGF method to several problems of alloy theory have shown that it is an excellent tool for studing systems with an arbitrary distribution of atoms on the sites of the underlying crystal lattice. The method allows one to include directly short range order effects when calculating the electronic structure and the total energy of random alloys. In particular, mixing energies of fcc Cu-Zn alloys calculated by the LSGF method for alloys with appropriate amount of short-range order were found to be in much better agreement with experiment than those where short-range order was neglected [8]. Moreover, the LSGF method takes into account all the local environment effects. Thus, it provides one with an atomic scale resolution when analyzing the electronic properties of materials, for example, spectral properties [37] or local magnetic moments [55].

The LSGF method gives one the opportunity to calculate the so-called effective cluster interactions which can be later applied in the framework of a statistical mechanical technique in order to study phase stabilities of alloys. In particular, one can extract *concentration dependent* effective cluster interactions.

This may be done by calculating the total energies of alloys with different sets of correlation functions but for some fixed concentrations of the alloy components and then by mapping these energies onto the corresponding cluster expansion. Since these calculations are fast one may perform a large number of them and thereby increase the accuracy of the interaction parameters obtained. The resulting effective cluster interactions will include all contributions to the total energy. Such calculations have been carried out with a great success by Simak *et al.* [9] for a multicomponent Cu_2NiZn alloy.

By means of the LSGF method one can also study properties of point defects and their clusters. In particular, in order to study a realistic metal-vacancy system, it is necessary to consider a large supercell in which the vacancies are well separated. To calculate vacancy-vacancy or vacancy-solute interaction energies in alloys or to study complex thermal defects in some intermetallics, very large supercells are necessary, so conventional methods of band structure calculations become extremely inefficient. Here our $O(N)$ technique has allowed us, for example, to perform a systematic study of the vacancy formation energy of the $3d$, $4d$, and $5d$ transition and noble metals, and to discuss its variation through a transition metal series, as well as the effects of crystal and magnetic structure [30], and the interaction of vacancies with other defects [10].

In conclusion, we find in number of applications and numerical tests that the LSGF method in conjunction with the TB-LMTO basis set leads to a reliable description of electronic properties of alloys. In general it yields results in excellent agreement with those obtained by alternative first-principles techniques, but becomes more efficient than the latter already for systems that contain 30 to 100 atoms in the unit cell. Thus, the LSGF method is a powerful technique for solving different problems of materials science theory.

Acknowledgements

This work has been partly supported by the Swedish Natural Science Research Council and by SKB AB, the Swedish Nuclear Fuel and Waste Management Company. The support by the TMR-network "Interface Magnetism" and by the Swedish Materials Consortium #9 are acknowledged. IAA is grateful to Dr. S. I. Simak for useful discussion of the manuscript. Collaboration with Dr. A. V. Ruban and Prof. H. L. Skriver in the development of the LSGF method is also acknowledged.

References

1. D. Pettifor, *Bonding and structure of molecules and solids* (Clarendon Press, Oxford, 1995).
2. F. Ducastelle, *Order and Phase Stability in Alloys* (North-Holland, Amsterdam, 1991).
3. B. Drittler, M. Weinert, R. Zeller, and P. H. Dederichs, Phys. Rev. B**39**, 930 (1989).
4. H. L. Skriver and N. M. Rosengaard, Phys. Rev. B **46** 7157 (1992).

5. A. Christensen, A. V. Ruban, P. Stoltze, K. W. Jacobsen, H. L. Skriver and J. K. Nørskov, Phys. Rev. B **56**, 5822 (1997).
6. P. Hohenberg and W. Kohn, Phys. Rev. **136B** 864 (1964).
7. W. Kohn and L.J. Sham, Phys. Rev. **140** A1133 (1965).
8. I. A. Abrikosov, A. M. N. Niklasson, S. I. Simak, B. Johansson, A. V. Ruban, and H. L. Skriver, Phys. Rev. Lett. **76**, 4203 (1996).
9. S. I. Simak, A. V.Ruban, I. A. Abrikosov, H. L. Skriver, and B. Johansson, Phys. Rev. Lett. **81**, 188 (1998).
10. P. A. Korzhavyi, I. A. Abrikosov, and B. Johansson, Acta Mater. **47**, 1417 (1999).
11. W. Kohn, Phys. Rev. Lett. **76**, 3168 (1996).
12. D. M. C. Nicholson, G. M. Stocks, Y. Wang, W. A. Shelton, Z. Szotek, and W. M. Temmerman, Phys. Rev. B **50**, 14686 (1994).
13. Y. Wang, G. M. Stocks, W. A. Shelton, D. M. C. Nicholson, Z. Szotek, and W. M. Temmerman, Phys. Rev. Lett. **75**, 2867 (1995).
14. W. Yang, Phys. Rev. Lett. **66**, 1438 (1991); T. Zhu, W. Pan, and W. Yang, Phys. Rev. B **53**, 12713 (1996).
15. G. Galli and M. Parrinello, Phys. Rev. Lett. **69**, 3547 (1992); F. Mauri, G. Galli, and R. Car, Phys. Rev. B **47**, 9973 (1993); F. Mauri and G. Galli, Phys. Rev. B **50**, 4316 (1994).
16. P. Ordejón, D. A. Drabold, M. P. Grumbach, and R. M. Martin, Phys. Rev. B **48**, 14646 (1993); P. Ordejón, D. A. Drabold, R. M. Martin, and M. P. Grumbach, Phys. Rev. B **51**, 1456 (1995); S. Itoh, P. Ordejón, D. A. Drabold, and R. M. Martin, Phys. Rev. B **53**, 2132 (1996), P. Ordejón, E. Artacho, and J. M. Soler, Phys. Rev. B **53**, R10441 (1996).
17. W. Kohn, Chem. Phys. Lett. **208**, 167 (1993).
18. E. B. Stechel, A. R. Williams, and P. J. Feibelman, Phys. Rev. B **49**, 10088 (1994); W. Hierse and E. B. Stechel, Phys. Rev. B **50** 17811 (1994).
19. X.-P. Li, R.W. Nunes, and D. Vanderbilt, Phys. Rev. B **47**, 10891 (1993).
20. M. S. Dow, Phys. Rev. B **47**, 10895 (1993).
21. S.-Y. Qiu, C. Z. Wang, K. M. Ho, and C. T. Chan, J. Phys.: Condens. Matter **6**, 9153 (1994).
22. E. Hernandez and M. J. Gillan, Phys. Rev. B **51** 10157 (1995); E. Hernandez, M. J. Gillan, and C. M. Goringe, Phys. Rev. B **53** 7147 (1996).
23. A. E. Carlsson, Phys. Rev. B **51**, 13935 (1995).
24. S. Goedecker and L. Colombo, Phys. Rev. Lett. **73**, 122 (1994); S. Goedecker and M. Teter, Phys. Rev. B **51**, 9455 (1995).
25. A. F. Voter, J. D. Kress, and R. N. Silver, Phys. Rev. B **53** 12733 (1996).
26. A. P. Horsfield, A. M. Bratkovsky, M. Fearn, D. G. Pettifor, and M. Aoki, Phys. Rev. B **53** 12694 (1996).
27. S. Baroni and P. Giannozzi, Europhys. Lett. **17**, 547 (1992).
28. I. A. Abrikosov, S. I. Simak, B. Johansson, A. V. Ruban, and H. L. Skriver, Phys. Rev. B **56**, 9319 (1997).
29. H. L. Skriver and N. M. Rosengaard, Phys. Rev. B **43** 9538 (1991).
30. P. A. Korzhavyi, I. A. Abrikosov, B. Johansson, A. V. Ruban, and H. L. Skriver, Phys. Rev. B **59**, 11693 (1999).
31. O. K. Andersen, Phys. Rev. B **12**, 3060 (1975).
32. O. K. Andersen and O. Jepsen, Phys. Rev. Lett. **53**, 2571 (1984).
33. O.K. Andersen, O. Jepsen, and D. Glötzel, in *Highlights of Condensed-Matter Theory* , edited by F. Bassani, F. Fumi, and M. P. Tosi (North Holland, New York, 1985).

34. O. Gunnarsson, O. Jepsen, and O. K. Andersen, Phys. Rev. B **27**, 7144 (1983).
35. H. L. Skriver, *The LMTO Method* (Springer-Verlag, Berlin, 1984).
36. J. S. Faulkner, Prog. Mater. Sci. **27**, 1 (1982).
37. I. A. Abrikosov and B. Johansson, Phys. Rev. B **57**, 14164 (1998).
38. J. S. Faulkner, N. Y. Moghadam, Y. Wang and G. M. Stocks, Phys. Rev. B **57**, 7653 (1998).
39. I. A. Abrikosov and B. Johansson, Philos. Mag. B **78**, 481 (1998).
40. R. Podloucky, R. Zeller, and P. H. Dederichs, Phys. Rev. B **22**, 5777 (1980); B. Drittler, M. Weinert, R. Zeller, and P. H. Dederichs, Phys. Rev. B**39**, 930 (1989).
41. C. Koenig, N. Stefanou, and J. M. Koch, Phys. Rev. B **33**, 5307 (1986).
42. D. D. Johnson, D. M. Nicholson, F. J. Pinski, B. L. Gyorffy, and G. M. Stocks, Phys. Rev. Lett. **56**, 2088 (1986); D. D. Johnson, D. M. Nicholson, F. J. Pinski, B. L. Gyorffy, and G. M. Stocks, Phys. Rev. B **41**, 9701 (1990).
43. I. A. Abrikosov and H. L. Skriver, Phys. Rev. B **47**, 16532 (1993).
44. A. V. Ruban, A. I. Abrikosov, and H. L. Skriver, Phys. Rev. B **51** 12958 (1995).
45. T. Beuerle, R. Pawellek, C. Elsässer, and M. Fähnle, J. Phys.: Condens. Matter **3**, 1957 (1991).
46. P. Braun, M. Fähnle, M. van Schilfgaarde, and O. Jepsen, Phys. Rev. B **44**, 845 (1991).
47. M. Sinder, D. Fuks, and J. Pelleg, Phys. Rev. B **50**, 2775 (1994).
48. B. Drittler, M. Weinert, R. Zeller, and P. H. Dederichs, Solid State Comm., **79**, 31 (1991).
49. P. H. Dederichs, B. Drittler, R. Zeller, Mater. Research Soc. Symp. Proc. **253**, 185 (1992).
50. A. V. Ruban, private communication.
51. W. Lambrecht and O. K. Andersen, Surface Sci. **178**, 256 (1986); Private communication
52. J. Kudrnovský, P. Weinberger, and V. Drchal, Phys. Rev. B **44**, 6410 (1991).
53. N. Papanikolaou, R. Zeller, P. H. Dederichs, and N. Stefanou, Phys. Rev. B **55**, 4157 (1997).
54. Z. W. Lu, S.-H. Wei, and A. Zunger, Phys. Rev. B **45**, 10314 (1992).
55. P. James, O. Eriksson, B. Johansson, and I. A. Abrikosov, Phys. Rev. B **59**, 419 (1999).